Chromospheric and Coronal Physics, Magnetic and Nonmagnetic Heating of the Outer Stellar Atmospheres

P.Ulmschneider

Institute for Theoretical Astrophysics, University of Heidelberg
Albert Überlestr. 2, D-69120 Heidelberg, Germany
Tel.: +49-6221-373776
FAX: +49-6221-372463
E-mail: ulm@ita.uni-heidelberg.de

Abstract

Practically all stars have chromospheres and coronae, that is, hot to very hot outer layers which are responsible for the UV-, X-ray and radio emissions and which are the origin and often cause for the stellar winds. Chromospheres are layers where the temperature rises from the stellar surface in outward direction to values of about 10 000 K while in the coronae the temperatures rise to millions of K.

The fundamental question is how are these layers heated to the high temperatures. Since the neighbors of most stars except for close binaries are far away and as the interstellar medium is very thin, this heating cannot come from outside the star but must originate from the stellar interior. It is the main goal of our group to clarify the heating mechanisms that produce chromospheres and coronae, and to use this knowledge to construct theoretical models of these outer layers.

Overview of our work on chromospheres and coronae

1. Chromospheres, coronae and the heating problem

One of the basic problems in astrophysics is to identify the heating mechanisms of chromospheres and coronae. In the reviews by Narain & Ulmschneider (1990, 1996), Ulmschneider (1996), Ulmschneider & Musielak (2003) it is shown that there are a large number of different heating mechanisms that can be classified as acoustic mechanisms (where acoustic waves are dissipated by shocks) and magnetic mechanisms. The magnetic mechanisms can be subdivided into wave mechanisms (AC-mechanisms) where magnetohydrodynamic (MHD) wave energy is guided by the magnetic field and dissipated by shocks, and current mechanisms (DC-mechanisms) where the energy stored in the magnetic field is dissipated by reconnection.

Since the discovery in the 1970's that short period acoustic waves could be responsible for the heating of the solar chromosphere (Ulmschneider 1970) and that the presence of such waves is indicated from the theoretically computed frequency spectra of acoustic waves, generated in the turbulent convection zone (Stein 1968), our group in a series of publications has attempted to predict the acoustic wave generation and studied in detail the shock wave heating by short period acoustic waves (e.g. Ulmschneider et al. 1978, Schmitz, Ulmschneider & Kalkofen 1985, Ulmschneider, Muchmore & Kalkofen 1987, Rammacher & Ulmschneider 1992, 2003, Fawzy et al. 2002a, b, c). In a similar way we calculated the generation of magnetohydrodynamic (MHD) waves in magnetic flux tubes and generated theoretical chromosphere models for stars that are covered by various amounts of magnetic fields (Huang, Musielak & Ulmschneider 1995, Ulmschneider & Musielak 1998, Ulmschneider, Musielak & Fawzy 2001, Cuntz et al. 1999, Fawzy et al. 2002a, b, c).

The great difficulty in deciding whether acoustic waves, MHD-waves or reconnection are important heating mechanisms for stellar chromospheres is, that despite of the close proximity of the Sun it is currently not possible to reliably differentiate between magnetic heating in unresolved fields on the Sun and acoustic dissipation. This

is because the spatial resolution of the solar surface is still insufficient for a reliable discrimination. Surprisingly it has turned out that by observing distant stars, which appear as mere point sources in the sky, it has become possible to progress significantly towards an answer to this question.

It is well known that models of the stellar interior can be computed by solving a system of 4 differential equations: the mass- and energy conservation equations (here the energy generation is by nuclear processes and by gravitational contraction), the hydrostatic equilibrium equation and an equation that describes the transport of energy from the stellar core through the stellar envelope by means of radiation and convection. These differential equations have to be augmented by equations describing material properties, the nuclear energy generation rate ϵ, the absorption coefficient for radiation κ and some thermodynamic quantities as functions of temperature T and gas pressure p.

One finds that exactly 3 free parameters uniquely specify the structure and evolution of a star model: the surface-metallicity of the stellar gas Z_M, the stellar mass M_* and the evolutionary time t_E that has elapsed since the star began its hydrogen burning. The last two parameters can be replaced by two surface parameters, the effective temperature T_{eff} and surface gravity g. The fact that the stellar interior depends on only the 3 independent parameters Z_M, T_{eff} and g is also valid for stellar photospheres, the regions that lie directly below the chromospheres and emit most of the visible light.

Since chromospheres and coronae owe their existence to the stellar interior, they therefore ought to depend only on 3 parameters. This is valid for cases where magnetic fields are not important. However, as magnetic fields dominate most chromospheres and certainly the coronae there is a fourth independent parameter, the stellar rotation period P_{Rot} that has to be specified because the mechanism that generates stellar magnetic fields, the dynamo mechanism, works only when convection and rotation are both present in a star.

A powerful method to clarify the relative importance of chromospheric and coronal heating mechanisms, in addition to a detailed comparison study of the individual mechanisms is, to observe how the chromospheric emission varies when the values of Z_M, T_{eff}, g and P_{Rot} change among the stars.
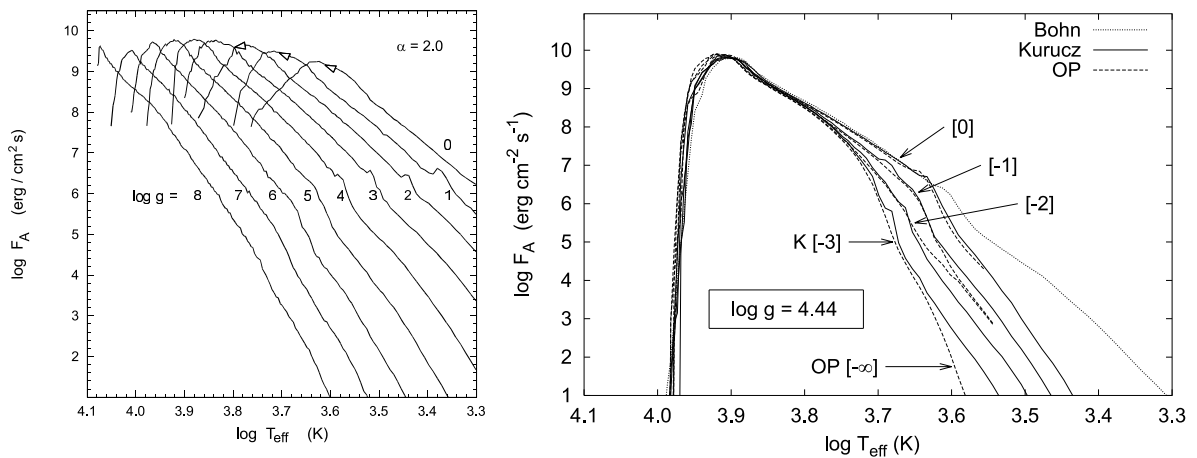

Fig. 1 Acoustic wave fluxes for main sequence and giant stars of solar abundance (left panel), after Ulmschneider, Theurer & Musielak (1996), as well as acoustic wave energy fluxes with non-solar metallicities (right panel), after Ulmschneider et al. (1999)

2. Acoustic wave energy flux calculations

For the computation of acoustic wave energy, rotation is unimportant since the convection zones are not affected much by rotation. This is different for the magnetic field generation and therefore magnetic heating, where because of the dynamo mechanism the coverage of the star by magnetic fields depends on the parameter P_{Rot}. Figure 1 shows the computed acoustic wave energy fluxes F_A on basis of convection zone models for stars where the parameters Z_M, T_{eff} and g are varied (Ulmschneider, Theurer & Musielak 1996, Ulmschneider et al. 1999). Figure 1a, where Z_M is held to solar values, shows that F_A varies enormously with T_{eff} and g. This is due to the very high dependence of the velocity of the convective gas bubbles with T_{eff} and g in the convection zones. Holding the surface gravity g to typical values for main sequence stars, Fig. 1b shows how acoustic fluxes vary with T_{eff} and different metal abundances of 1/1, 1/10, 1/100 and 1/1000 solar metallicity ($Z_M = [0], [-1], [-2], [-3]$). For cool stars the drop of F_A is explained by the fact that the decreasing metal abundance decreases the opacity which allows the stellar surface (from where the main body of the stellar radiation escapes) to occur at deeper layers in the star where the convective velocities are much smaller. For hotter stars this effect is decreased or absent because the opacity there is mainly due to hydrogen and not to metals, it is therefore insensitive to variations of Z_M.

3. Theoretical chromosphere models based on acoustic heating

Generated in the top parts of the stellar convection zones acoustic waves propagate in all directions. Those waves that propagate upwards to the stellar surface and into the photosphere encounter the rapidly decreasing density of the outer layers of the stars. Like water waves on the sea shore the acoustic wave amplitudes in this case grow rapidly (due to the conservation of the acoustic flux) which leads to the formation of shocks. Shocks are a very efficient way to dissipate the acoustic wave energy. Since chromospheres owe their existence to heating we suggest that acoustic wave heating is responsible for the generation of chromospheres.

The problem is how to do a realistic simulation of the acoustic wave propagation and shock formation. The waves are a spherical phenomenon and the density decreases only in vertical direction. In addition, an entire spectrum of acoustic waves is generated and individual wave frequencies behave differently in the shock formation process. Moreover, one has complicated effects of departures from thermodynamic equilibrium (NLTE) for the gas and time-dependent effects in the ionization of hydrogen and metals. In the outer stellar atmosphere these effects are of prime importance because near the stellar surface the radiation is very unisotropic, coming only from the direction of the star and because these layers have low density. With vastly increased future computer power fully realistic simulations of the wave propagation of an acoustic spectrum under such conditions emanating from many sources on the star will be no problem. However, at the present time only a highly simplified wave calculation is possible.

For this reason we use a one-dimensional (1D) time-dependent radiation-hydrodynamic code that treats the acoustic waves as plane waves which propagate only in the vertical direction. With such a code it is possible to follow the propagating acoustic wave into the chromosphere where shock formation and shock dissipation take place. The acoustic waves are introduced at the bottom of an initial stellar atmosphere model by specifying the velocity at a piston. Since an acoustic spectrum would lead to frequent shock mergings which generates large unobserved shocks which is an artifact of the plane-parallel wave treatment (Ulmschneider et al. 2005) we represent the acoustic wave spectrum by a monochromatic wave with a suitably chosen wave period P that represents the peak of the acoustic spectrum. For P we choose P$\approx$ $P_A/5$ to $P_A/10$ where P_A is the acoustic cut-off period and the amplitude of the velocity fluctuation at the piston
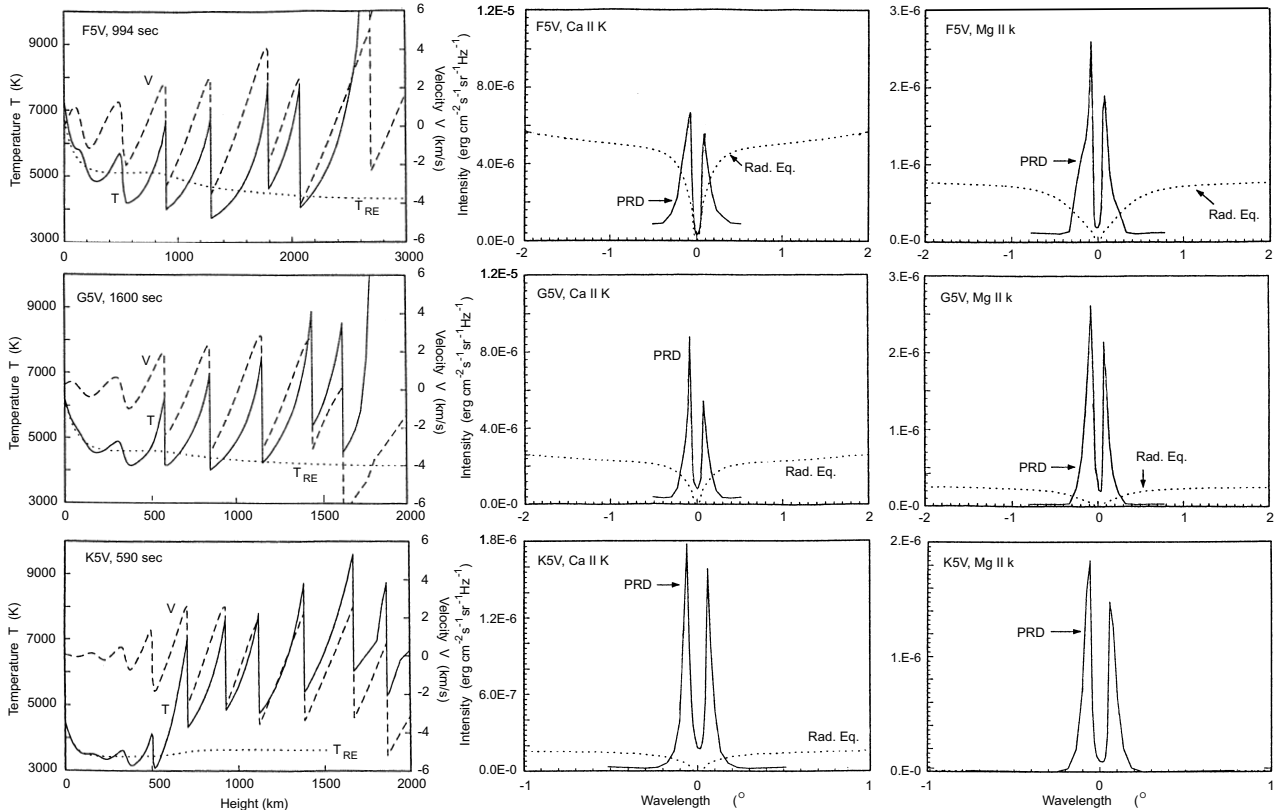
Fig. 2 Chromosphere models with monochromatic acoustic waves showing temperature T and velocity V fluctuations and the development of shocks (left panels). The middle panels show the corresponding Ca II K line profiles and the right panels the Mg II k profiles, after Buchholz & Ulmschneider (1994)

is determined from the acoustic flux F_A. The initial atmosphere model was chosen to be in radiative equilibrium because the atmosphere should not show motion before the waves are introduced.

Figure 2 shows such wave computations and chromosphere models for three main sequence stars (of spectral class F5V, G5V, K5V), after Buchholz & Ulmschneider (1994). On basis of these models the emerging Ca II and Mg II resonance line fluxes were computed allowing for partial frequency redistribution (PRD) (Ulmschneider 1994). By integrating these line core emission fluxes over frequency (the other parts of the lines were not simulated), total line fluxes (Ca II H+K, Mg II h+k) were computed and compared with observations. In the left panels it is seen that during propagation through the photospheric layers the waves grow in amplitude and form shocks which give rise to intense mechanical heating. This raises the mean temperatures and generates the chromospheres.

4. Comparison with observations

The observed radiation flux in the emission cores of the chromospheric spectral lines of Ca II and Mg II of slowly rotating stars (stars which are not dominated by magnetic fields), occupy a so-called *basal flux limit* line in a diagram of the observed emission flux versus T_{eff} (or color index B-V) (see Fig. 3). It is thought that the more emission a star has relative to the basal flux limit, the more rapid it rotates and the more it is covered by magnetic fields and affected by magnetic heating. Observationally it is found that all nonmagnetic stars occupy essentially the same basal flux curve, regardless of whether they are giants (low gravity) or dwarfs (high gravity) or whether they have solar metal
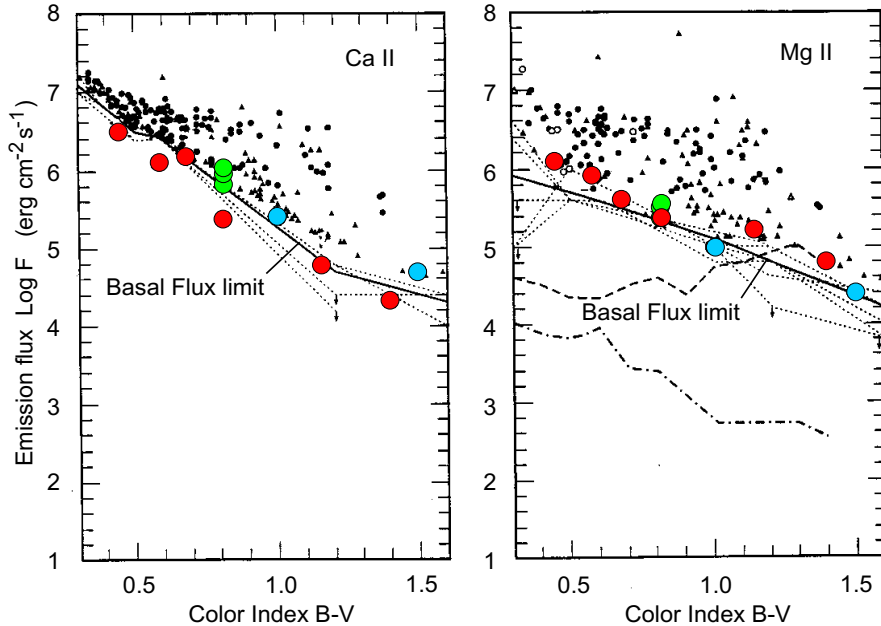
Fig. 3 Comparison of the chromospheric line core emission fluxes from acoustically heated theoretical chromosphere models with observations of Ca II and Mg II lines by Rutten et al. (1991). The basal flux curve is shown drawn. Red dots mark main-sequence stars of solar abundances, blue dots giant stars of solar abundances, while green dots giants with 1/1, 1/10 and 1/100 solar abundances, after Cuntz, Rammacher & Ulmschneider (1994) and Buchholz, Ulmschneider & Cuntz (1998)

abundance or 1/100 solar metal abundance.

Figure 3 shows observations by Rutten et al. (1991) together with our simulations of main sequence stars, giants and low metallicity stars (Cuntz, Rammacher & Ulmschneider 1994, Buchholz, Ulmschneider & Cuntz 1998). It is surprising that despite our crude approach the theoretical values are not only in the vicinity of the observations but that they actually lie near the basal flux line which they should because we did not take magnetic heating effects into account. What is even more surprising (in view of the enormous T_{eff} dependence seen in Fig. 1a) is that the slope of the basal flux line versus B-V is nicely reproduced as well as the observational fact that the giants and low metallicity stars have the same basal flux line. This is taken by us as a strong indication that the acoustic heating model for slowly rotating stars appears to be valid. In other words, acoustic waves are identified as the main heating mechanism for nonmagnetic chromospheres. This view, however, has to be confirmed with much more sophisticated and realistic simulations of acoustic wave propagation in the future.

5. Magnetohydrodynamic wave energy generation

As our approach for nonmagnetic chromospheres led to encouraging results, is it possible to extend it to magnetic cases? Empirically it is known that the more rapidly a star rotates, the more densely it is covered by magnetic fields (Rutten 1986, Schrijver et al. 1989, Cuntz, Ulmschneider & Musielak 1998). At the present time there are intense efforts to develop a dynamo theory to enable to predict the magnetic field coverage of stars with different rotation periods P_{Rot}, but such a tool is not yet available. Other than to employ empirical relations, a way to proceed is therefore to simply assume a filling factor f for the magnetic field (f is the ratio of the area covered by magnetic flux to the total surface area of the star) and then look what consequences the assumed
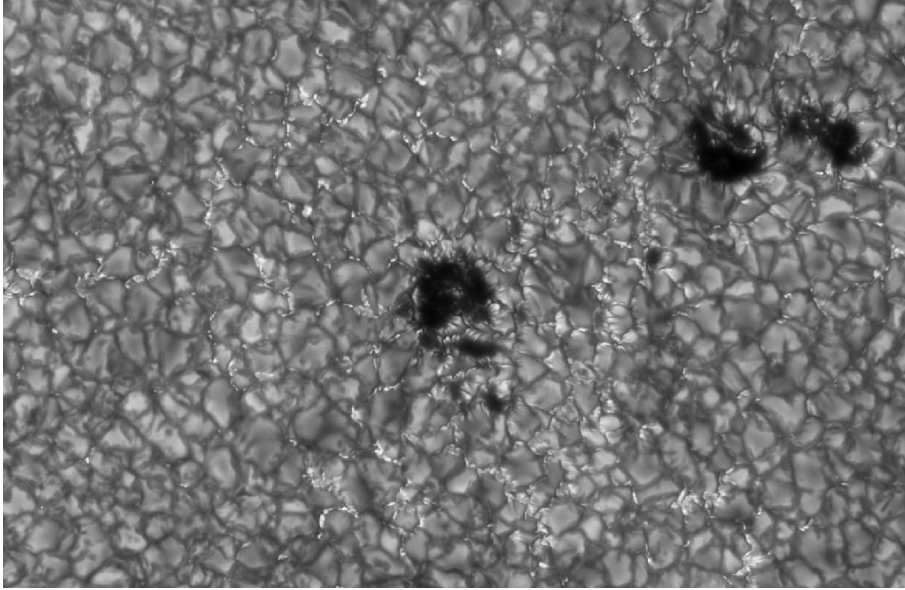
Fig. 4 Granulation on the solar surface. Granules are hot gas bubbles that rise up from the convection zone to the solar surface where they cool and after lifetimes of a few minutes vanish again. Small white specs called filigree are seen that are signatures of magnetic flux tubes. They are found in the dark intergranular lanes where the cooled gas converges and flows back down into the convection zone. Also seen are small sunspots (dark spots). The picture is from the Swedish Solar Tower at La Palma

variation of f has for the chromospheric emission. We hope that in the near future a dynamo theory will be available which, after specifying the 4 parameters Z_M, T_{eff}, g and P_{Rot}, will give us a unique value of the filling factor f for the star.

To proceed with an assumed f, a number of additional assumptions has to be made. While the most noticeable magnetic feature on the Sun are sunspots, most of the magnetic flux arises in small magnetic elements called magnetic flux tubes. Recent very high resolution images of the solar granulation (Fig. 4) show that these magnetic elements are distributed everywhere over the solar surface, they are noticeably concentrated near the boundaries of supergranulation cells and are located in the dark intergranular lanes between granules where the cool gas of the upwelling granular bubbles flows back down into the solar interior. These magnetic elements are signatures for magnetic flux tubes, bundles of magnetic field in an otherwise field-free surroundings that emerge vertically from the deeper layers. The vertical orientation of the flux tubes is due to buoyancy because as a consequence of horizontal pressure balance between magnetic and gas pressures one has much lower gas pressure inside the tube.

Another assumption that has to be made is about the value of the magnetic field strength B inside the flux tube. If there is essentially no gas inside the tube then the external gas pressure p_E is equal to the magnetic pressure in the tube $p_E = B_{EQ}^2/8\pi$, where B_{EQ} is the equilibrium field strength. But realistic tubes are not empty and therefore one must have $B < B_{EQ}$. MHD-simulations of the convective collapse of gas in a magnetic flux tube reveal the true value of the field strength B and the amount of gas pressure left in a given tube. However, as such calculations are not yet available for arbitrarily specified stellar parameters we assume that one has typical solar conditions where the tubes have a range of field strengths $B/B_{EQ} = 0.75, 0.85, 0.95$ (Ulmschneider, Musielak & Fawzy 2001).

We therefore picture the star as covered by a large amount of magnetic flux tubes, consistent with an assumed value of f (Fig. 5), which at the stellar surface have diameters of roughly a scale height H and a field strength given by $B/B_{EQ} \approx 0.85$. These
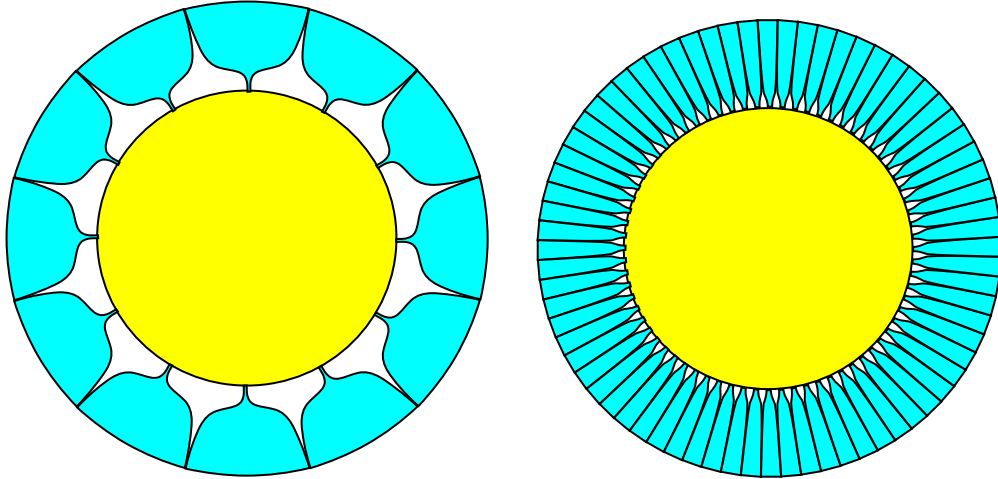
Fig. 5 Magnetic flux tubes on stars with different magnetic filling factors. Left: star with a low filling factor, there are few tubes on the star. Right: star with a high filling factor. The magnetic fields (blue) spread until they fill out the entire available space

tubes subsequently spread with height according to horizontal pressure balance and at a certain height completely fill out the available space. The flux tubes go down into the convection zone and it is imagined that they are perturbed by the gas motions that take place in the nonmagnetic regions outside the tubes. By these perturbations three types of MHD-waves are generated. Squeezing the tube generates longitudinal waves, shaking the tube produces transverse waves and twisting the tube gives rise to Alfvén waves (Fig. 6).
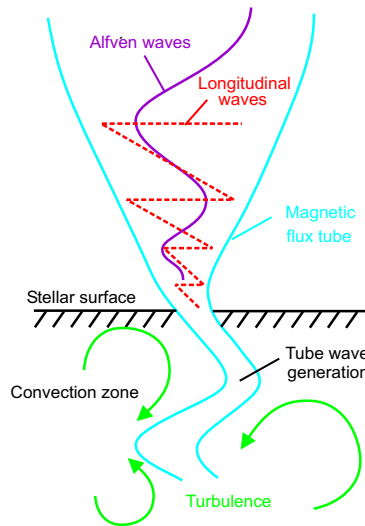

Fig. 6 Magnetohydrodynamic wave generation in magnetic flux tubes when turbulent convection bends and compresses the tubes

By letting time-dependent pressure oscillations or horizontal velocity fluctuations driven by Kolmogorov turbulence act on magnetic flux tubes, the longitudinal or transverse Alfvén wave energy generation can be computed. Figure 7 shows the longitudinal wave energy flux for stars of different T_{eff} and g (Ulmschneider & Musielak 1998, Ulmschneider, Musielak & Fawzy 2001), assuming solar metallicities and various ratios of B/B_{eq}. For similar calculations for transverse Alfvén waves see Huang, Musielak & Ulmschneider (1995), Musielak & Ulmschneider (2001, 2002a, b).
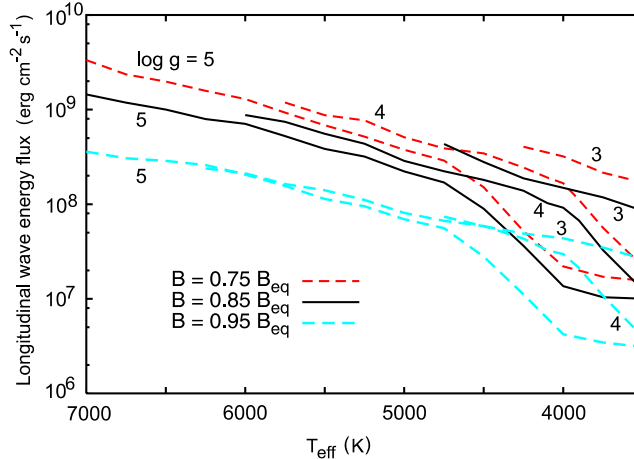
7

Fig. 7 Longitudinal tube wave fluxes for stars versus T_{eff} for given $\log g$, with solar metallicity $Z_m = [0]$, $\alpha = 2$ and different ratios of magnetic field strength B_0/B_{eq}, after Ulmschneider, Musielak & Fawzy (2001)

6. Magnetic chromospheres

To compute MHD-waves along magnetic flux tubes one can again use a simple 1D time-dependent radiation-hydrodynamic code where the tube model is pictured as a stack of mass elements that are connected but can individually move in three dimensions. This so-called thin flux-tube approximation, where the physical variables do not vary much over the tube cross-section and are given by the values at the tube center, is a very simple approximation and gives reasonable results compared to a more realistic treatment of the flux tube (Hasan & Ulmschneider 2004a, b). The waves are introduced at the bottom of the tube by specifying different types of longitudinal or transverse velocities on basis of the given wave energy flux and the assumed wave period.

The heating of magnetic tubes does not only depend on the available wave energy flux but also on the spreading of the tube, that is, on how quickly the tube cross-section increases with height. In Fig. 8 from Fawzy, Ulmschneider & Cuntz (1998) it is seen that for three tubes of different geometry the shock dissipation behaves differently. These tubes have the same cross-section at the bottom, the same wave energy input, and the same wave period of 20 s. There essentially is no heating in the exponential tube because the available wave energy is spread over a rapidly increasing cross-section and only very weak shocks form.

The constant cross-section tube has maximum heating. The wineglass tube geometry, which at at 1300 km height reaches a constant cross-section, is the most realistic case for magnetic regions. This maximum cross-section at the top of the tube is enforced by the other tubes which surround an individual tube. Since all tubes spread with height, they can only spread until all the available space is filled. Therefore, for a specified filling factor f the spreading of the flux tube model (Fig. 5) is important for the predicted wave heating.

To compare the chromosphere of a magnetic star with observations one has to simulate the core emission of the Ca II and Mg II lines. The flux tube geometry on stars with different filling factors and the ray paths used in the computation of the emergent intensity is shown in Fig. 9.

For a first application of our MHD-wave heating picture of magnetic chromospheres we selected K0V to K3V main sequence stars as a test case where the relationship between the magnetic flux and the rotation period, that is, the filling factor f as function of P_{Rot}, is known from observations. There are two effects that affect the heating in stars of the same spectral type but different rotation periods. The magnetic field strength B at the stellar surface on the stars in every flux tube is the same because it is related to
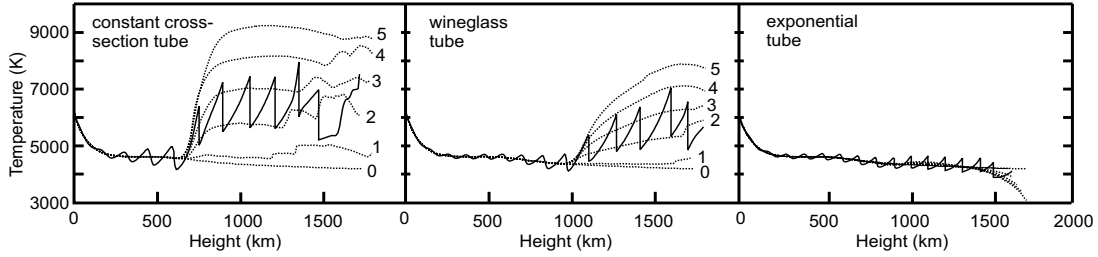
Fig. 8 Shock wave heating by an adiabatic wave of period 20 s in magnetic flux tubes of different geometry: Constant cross-section tube (left), wine glass tube (center), exponentially spreading tube (right). Mean values from 0 to 5 are shown dotted in 400 s intervals, after Fawzy, Ulmschneider & Cuntz (1998)
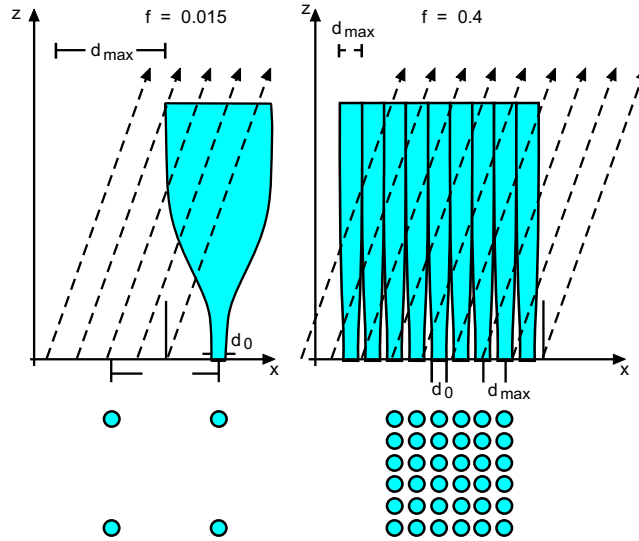

Fig. 9 Ray-paths through the forest of flux tubes for the computation of the emergent line radiation from stars with different magnetic filling factors f, after Cuntz et al. (1999) and Fawzy et al. (2002b). The arrangement of the tube cross-sections on the stellar surface is shown at the bottom

the gas pressure at the stellar surface which does not change with P_{Rot}, but the number of tubes and the amount of spreading is different (see Fig. 5). For each star we therefore have a flux tube model with the same cross-section at the stellar surface but different spreading in which the same computed longitudinal wave energy flux is introduced. We also assume that 10% of the transverse wave flux is converted to longitudinal wave flux due to mode-coupling.

Figure 10 shows the comparison of our simulations with observations for the Ca II H+K line core emission (Cuntz et al. 1999). It is seen that the observed rotation-chromospheric emission correlation is reasonably well reproduced. This may indicate that we have correctly identified the magnetic heating mechanism of chromospheres as MHD-waves.

For a more reliable identification of the MHD-wave heating picture of magnetic chromospheres this type of approach was carried out for many other stars and spectral lines (Ulmschneider et al. 2001, Fawzy et al. 2002a, b, c). Figure 11 shows the simulated Ca II core emission based on MHD-wave heating for main sequence stars of different assumed filling factors f with observations. It is seen that with increasing f the observed range between the basal flux limit and the saturation limit is essentially covered. Here we have limited f at a maximum value of f = 0.4 because as seen in Fig. 9 the flux tubes for that case still leave enough non-magnetic external space in the convection zone for the external turbulent motions to generate the MHD-wave energy. Since for higher
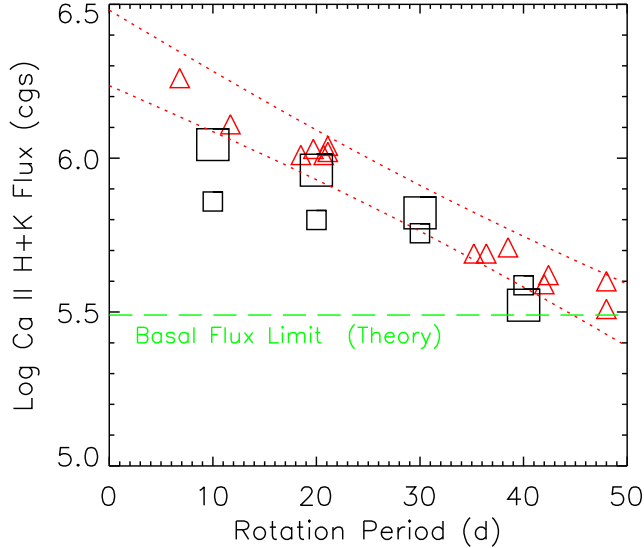
Fig. 10 Ca II H+K emission flux as function of stellar rotation, after Cuntz et al. (1999). The triangles give the observations for a set of stars with spectral type between K0V and K3V, which constitutes the empirical rotation-chromospheric emission relation. The squares indicate the results from two-component theoretical chromosphere models. The basal flux limit from pure acoustic heating is indicated
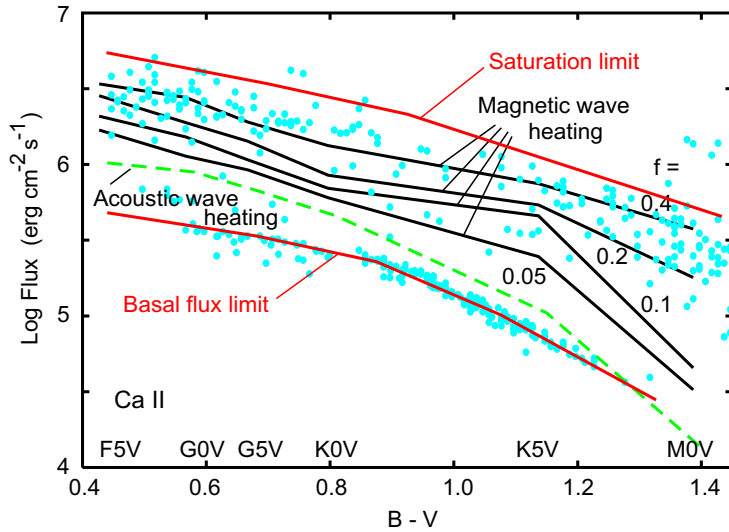

Fig. 11 Observed chromospheric Ca II H+K line core emission fluxes of individual stars compared with theoretical simulations based on MHD-wave heating in stars covered by different amounts of magnetic flux specified by the magnetic filling factor f, after Fawzy et al. (2002b)

values of f the convective motions and therefore the MHD-wave generation are thought to be impared, the case $f \approx 0.4$ should give the maximum MHD-wave generation in stars.

Figures 12 and 13 show for the Ca II H+K and Mg II h+k lines the maximum MHD-wave heating with filling factors $f = 0.4$ but different amounts of transverse wave heating added on top of the longitudinal wave heating. Since the transverse wave energy fluxes are much higher than the longitudinal wave fluxes we have multiplied the longitudinal fluxes by a factor M to take into account the conversion of transverse wave energy to longitudinal energy by mode-coupling. It is seen that the additional energy does not change the picture much. If we trust our crude methods it can be seen that while the
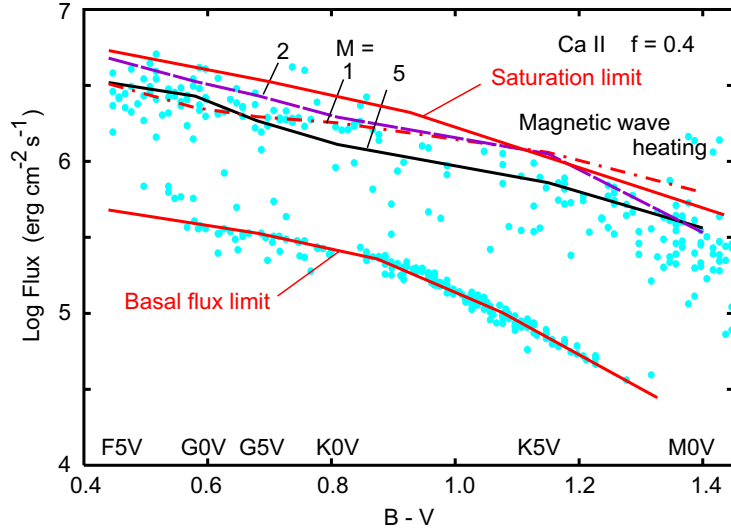
Fig. 12 Ca II H+K emission core flux observations in comparison with theoretical simulations with different amounts of maximum wave energy present when the magnetic filling factor is f = 0.4. Mode-coupled transverse wave energy is assumed to increase the longitudinal wave flux by the indicated factors M, after Fawzy et al. (2002b)
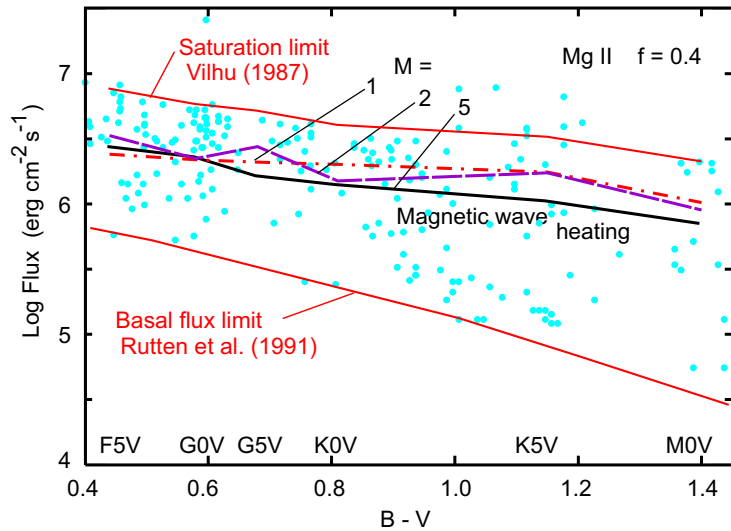

Fig. 13 Mg II h+k emission core observations in comparison with theoretical simulations with different amounts of maximum wave energy present when the magnetic filling factor is f=0.4. Mode-coupled transverse wave energy is assumed to increase the longitudinal wave flux by the indicated factors M, after Fawzy et al. (2002b)

Ca II saturation limit is reasonably well reproduced there seems to be a heating gap for the Mg II saturation limit. This may be due to our simple approach or could point to the neglected heating by magnetic field reconnection. This latter heating mechanism is supposed to become more important in higher layers (compared to the Ca II formation heights) where the Mg II line cores are formed and particularly in the corona. Another reason might be the crude handling of the mode-coupling with the much more energetic transverse waves.

7. Problems with wave observations on the Sun

When comparing velocity and intensity fluctuations in spectral lines with theoretical

acoustic spectra, an important effect must be considered. Velocity fluctuations can only be measured using spectral lines and by observing the Doppler effect (frequency fluctuations) in the absorption core of the line (Fig. 14). Strong lines form at great height and weak lines near the solar surface. If one wants to measure the velocity spectrum of acoustic waves produced in the convection zone one thus takes for instance a weak Fe line as it probes the deepest layers close to the convection zone. However, the formation even of weak lines requires a height interval over which the line contribution function is significant. This width is about two scale heights $\Delta z = 2 H \approx 300$ km. When the wavelength of the acoustic waves is smaller than Δz, then the line core does no longer show frequency fluctuations but only line broadening.
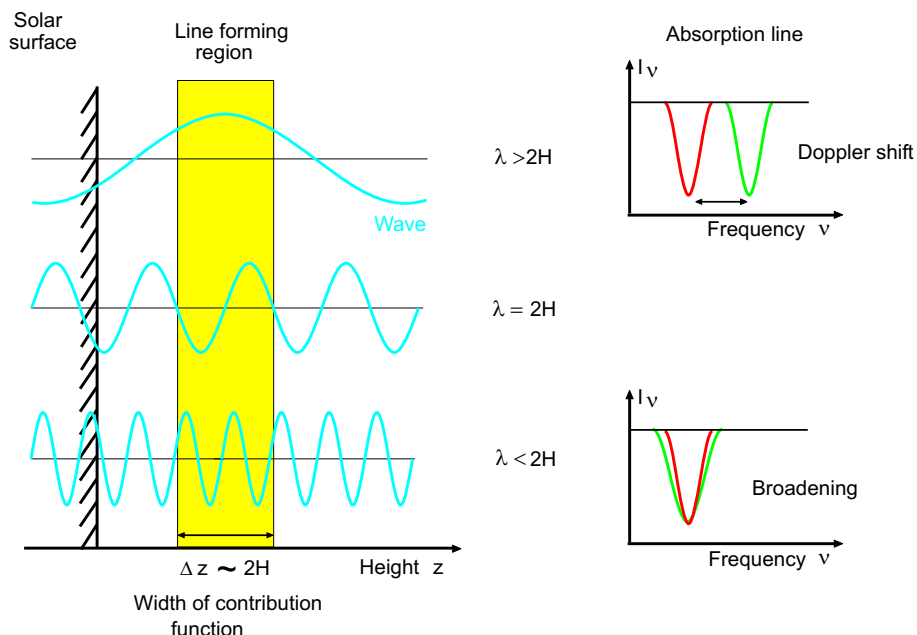

Fig. 14 Acoustic waves of different frequency propagate through the line forming region of a weak Fe line. The observed Doppler fluctuations depend on the ratio of the wavelength and the width of the line forming region
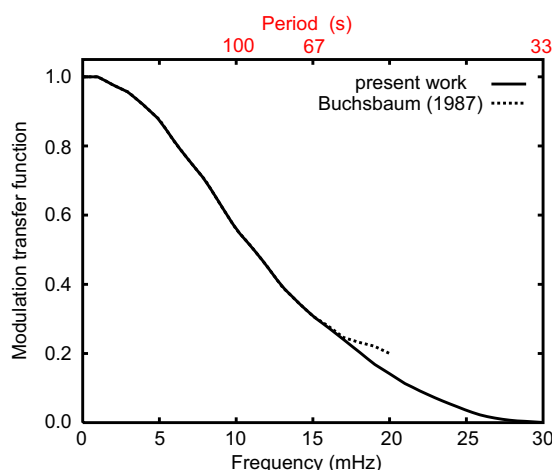

Fig. 15 The modulation transfer function gives the fraction of the velocity amplitude (the ratio of the observed to the actually present amplitudes) that can be observed of acoustic waves of various frequencies. Due to the finite extent of the line-formation region there is a certain frequency above which the waves can no longer be detected, after Theurer, Ulmschneider & Kalkofen (1997)

12

Assume that acoustic waves of different periods but with the same velocity amplitude (energy flux) are present on the Sun. What would we observe? This question is answered by the modulation transfer function MTF (Fig. 15) which tells how much of the velocity amplitude of a given wave frequency $\nu = 1/$period can be observed. One finds (Endler & Deubner 1983) that waves with periods of less than about 44 s ($= 2H/c_S = 300/7$ with a sound speed of $c_S = 7$ km/s) or frequencies higher than roughly $\nu = 23$ mHz cannot be observed because of the mentioned principal reasons. Figure 15 shows that even the velocity amplitudes of waves below this frequency are strongly reduced. We applied this MTF concept to our wave generation calculations and simulated the acoustic spectrum that might be observed from Earth.

Figure 16 shows a calculation where the acoustic wave spectrum computed in the solar convection zone at -160 km height is followed upwards to the height of 250 km (Musielak, Rosner, Stein & Ulmschneider 1994, Theurer, Ulmschneider & Kalkofen 1997) where observations of a low lying Fe line have been reported. Applying the MTF to the original spectrum and to the spectrum at 250 km height (red) shows that less than 10% of the actually present wave energy can be observed in the Fe line. Using only the observed power, the mechanical heating of the chromosphere would be greatly underestimated. In addition the observed low-frequency spectrum would predict only long period type phenomena, that is, the chromosphere would appear to be dominated by solitary long-period (3 min) type shock waves. Such strong single shocks are present in the solar chromosphere because the true acoustic spectrum contains these long period components, but they are not the only phenomena.
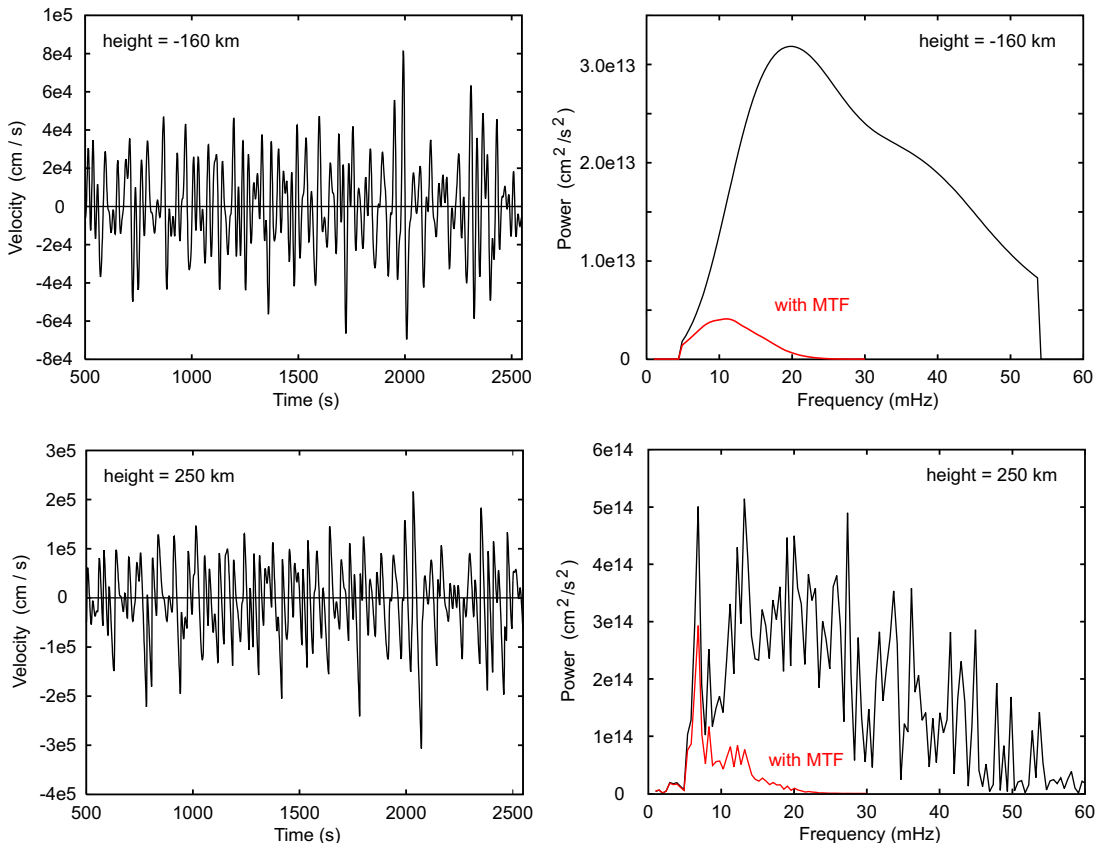

Fig. 16 Acoustic wave fluctuations and acoustic spectrum computed in the convection zone at the height -160 km (top). Velocity fluctuations and the spectrum after propagation of the wave to the height 250 km (bottom). At each height the spectrum after applying the MTF is shown in red, after Theurer, Ulmschneider & Kalkofen (1997)
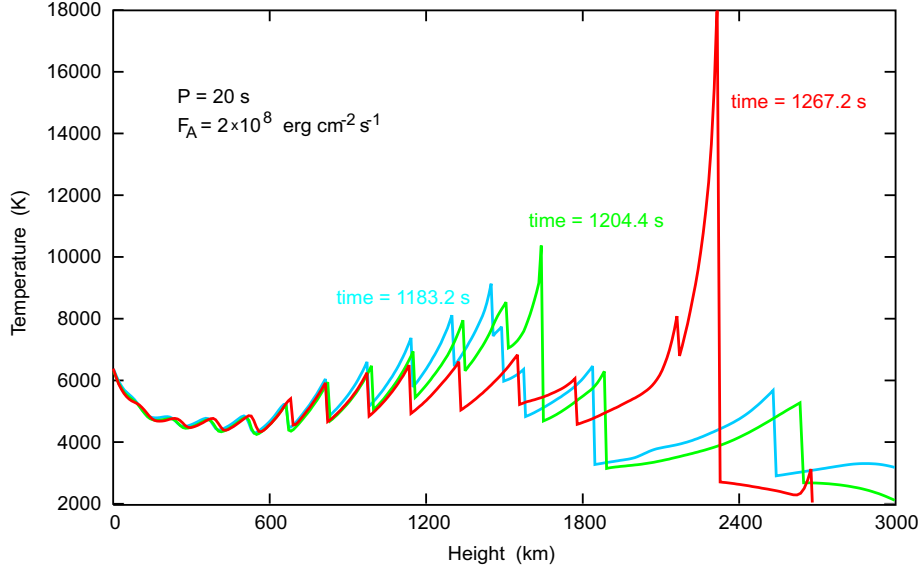
13

Fig. 17 Temperatures of three phases of an acoustic wave calculation in the solar atmosphere. The waves have a period of 20 s and the time of the phases is indicated
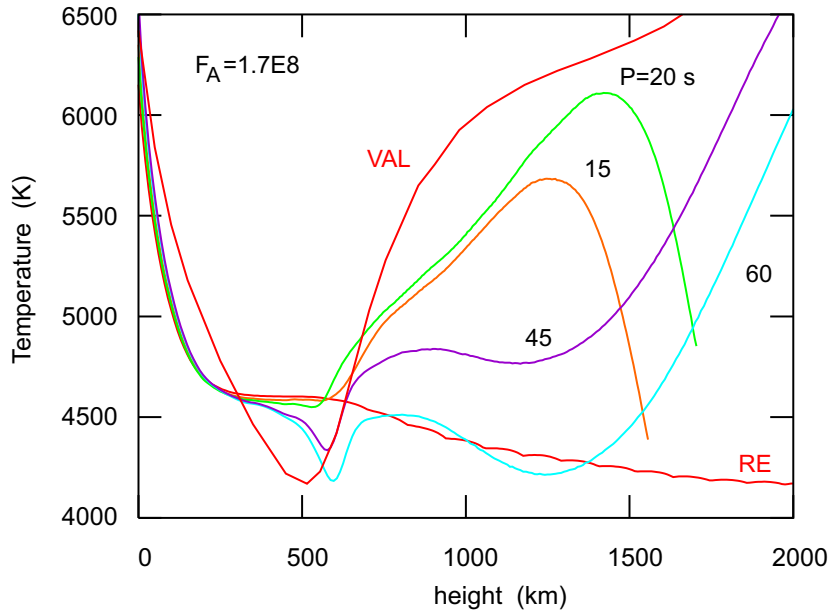

Fig. 18 Time-averaged temperatures in the solar atmosphere produced by monochromatic acoustic waves of different periods P but the same energy flux of $F_A = 1.7 \ 10^8$ erg cm^{-2} s^{-1}. Also shown is the initial radiative equilibrium temperature distribution before the waves started. VAL indicates the semiempirical model by Verazza, Avrett & Loeser (1981).

8. Problems with the acoustic wave heating

Figure 17 shows three phases of a monochromatic acoustic wave calculation in the solar atmosphere with a period of 20 s. The green phase is nearly one period later than the blue one and the red about 3 periods later than the green phase. This shows by the fact that at low height the three phases are almost identical. Near 1500 km height it is seen that three shocks merge between the blue and the green phases and that this shock merges with another until in the red phase it becomes very strong. The perpetual merging lets the shock grow rapidly in strength (and speed) and produces pronounced adiabatic cooling in the region behind it. This behavior repeats itself and causes the

14

time-averaged temperature to drop at this height as can be seen in Fig. 18.

Below the height of 1500 km the theoretical chromospheric temperature rise in outward direction shows a fair resemblance with the semiempirical atmosphere model by Verazza, Avrett & Loeser (VAL, 1981), which based on the observation of many continua (see Fig. 18) also features an outward chromospheric temperature rise. However, the disparant behavior above that height does not agree with the idea of acoustic heating of chromospheres. It was realized that the excessive numbers of shock mergings are an artifact of the 1D plane-parallel wave propagation and thus are caused by the inadequate use of our 1D mathematical code to simulate the acoustic wave propagation (Ulmschneider et al. 2005). Only in this very special 1D geometry are shocks so precisely aligned with each other that mergings occur between shocks that have shock jump regions with widths of the order of only meters and extend horizontally over hundreds or thousands of km.

In realistic situations where acoustic energy comes from extended and multiple sources distributed over the star is it very unlikely that occasional shock encounters will see shocks that are so precisely aligned that they merge. Much more likely is the situation that shock encounters will lead to a harmless crossing of shock fronts that are inclined against one another. Moreover, in a realistic 3D wave calculation the waves would propagate in every direction and we would frequently see shocks moving in non-vertical directions and directions other than the line of sight. Also, a frequent and persistent occurrence of strong shocks is not observed in chromospheres.

For this reason it is unavoidable that serious efforts must be made to go to 3D simulations which, however, must not neglect NLTE and time-dependent ionization effects. For this, massive computer power will be required.

Literature

Buchholz B., & Ulmschneider P., 1994, in: Cool Stars, Stellar Systems and the Sun, Caillault J.P., Ed., ASP Conf. Series 64, 363

Buchholz B., Ulmschneider P., & Cuntz M., 1998, ApJ 494, 700

Buchsbaum G., 1987, Diplom thesis, Univ. Würzburg, Germany

Cuntz M., Rammacher W., & Ulmschneider P., 1994, ApJ 432, 690

Cuntz M., Rammacher W., Ulmschneider P., Musielak Z.E., & Saar S.H., 1999, ApJ 522, 1053

Cuntz M., Ulmschneider P., & Musielak Z.E., 1998, ApJ 493, L117

Endler F., & Deubner F.-L., 1983, A&A 121, 291

Fawzy D.E., Ulmschneider P., & Cuntz M., 1998, A&A 336, 1029

Fawzy D., Rammacher W., Ulmschneider P., Musielak Z.E., & Stępień K., 2002a, A&A 386, 971

Fawzy D., Ulmschneider P., Stępień K., Musielak Z.E., & Rammacher W., 2002b, A&A 386, 983

Fawzy D., Stępień K., Ulmschneider P., Rammacher W., & Musielak Z.E., 2002c, A&A 386, 994

Hasan S.S., & Ulmschneider P., 2004a, A&A 422, 1085

Hasan S.S., & Ulmschneider P., 2004b, A&A 428, 1017

Huang P., Musielak Z.E., & Ulmschneider P., 1995, A&A 297, 579

Musielak Z.E., Rosner R., Stein R.F., & Ulmschneider P., 1994, ApJ 423, 474

Musielak Z.E., & Ulmschneider P., 2001, A&A 370, 541

Musielak Z.E., & Ulmschneider P., 2002a, A&A 386, 606

Musielak Z.E., & Ulmschneider P., 2002b, A&A 386, 615

Narain U., & Ulmschneider P., 1990, Space Science Reviews 54, 377

Narain U., & Ulmschneider P., 1996, Space Science Reviews 75, 453

Rutten R.G.M., 1986, A&A 159, 291

Rutten R.G.M., Schrijver C.J., Lemmens A.F.P., & Zwaan C., 1991, A&A 252, 203

Schrijver C.J., Coté J., Zwaan C., & Saar S.H., 1989, ApJ 337, 964

Rammacher W., & Ulmschneider P., 1992, A&A 253, 586

Rammacher W., & Ulmschneider P., 2003, ApJ 589, 988

Schmitz F., Ulmschneider P., & Kalkofen W., 1985, A&A 148, 217

Stein R.F., 1968, ApJ 154, 297

Theurer J., Ulmschneider P., & Kalkofen W., 1997, A&A 324, 717

Ulmschneider P., 1970, Solar Physics 12, 403

Ulmschneider P., 1994, A&A 288, 1021

Ulmschneider P., 1996, in: Cool Stars, Stellar Systems and the Sun, Astr. Soc. Pacific Conf. Ser. 109, Pallavicini R. and Dupree A.K. Eds., p. 71

Ulmschneider P., Muchmore D., & Kalkofen W., 1987, A&A 177, 292

Ulmschneider P., & Musielak Z.E., 1998, A&A 338, 311

Ulmschneider P., & Musielak Z.E., 2003, in: Current Theoretical Models and High Resolution Solar Observations: Preparing for ATST, ASP Conference Series Vol. 286, A.A. Pevtsov and H. Uitenbroek, Eds., p. 363

Ulmschneider P., Musielak Z.E., & Fawzy D.E., 2001, A&A 374, 662

Ulmschneider P., Rammacher W., Musielak Z.E., & Kalkofen W., 2005, ApJ 631, L155

Ulmschneider P., Schmitz F., Kalkofen W., & Bohn H.U., 1978, A&A 70, 487

Ulmschneider P., Theurer J., & Musielak Z.E., 1996, A&A 315, 212

Ulmschneider P., Theurer J., Musielak Z.E., & Kurucz R., 1999, A&A 347, 243

Vernazza J.E., Avrett E.H., Loeser R., 1981, ApJS 45, 635

Vilhu O., 1987, in: Cool Stars, Stellar Systems, and the Sun, J.L. Linsky & R.E. Stencel, Eds., Springer, Berlin, p. 110